Research on Passive Gamma Emission Tomography Method for Corrosion Detection of Liquid Lead-Bismuth Coolant

Yuhan Feng [1] Yixin Dong [1] Yongfei Liang [1] Lixin Bai [1] Bangyang Xia[2]
Chaowen Yang [1,*]

Affiliations:

[1]College of Physics, Sichuan University, Chengdu 610065, China

[2]Nuclear Power Institute of China, Chengdu 610213, China

[*]Corresponding author. *E-mail address:* ycw@scu.edu.cn

Abstract: Lead-cooled fast reactors are considered the next generation of nuclear reactors. One of the main challenges in developing lead-based fast reactors is the corrosion of structural materials by the liquid lead-bismuth coolant, as well as the formation of oxide particulates.It is an urgent need to develep a high-resolution non-destructive testing method for the detection of oxides and corrosion in pipeline of liquid lead-bismuth coolant. This paper investigates the feasibility of passive gamma emission tomography (PGET), a technique that utilizes gamma rays emitted by the lead-bismuth coolant, which is activated by neutrons in the reactor core, to inspect the lead-bismuth coolant pipelines corrosion. A simulation model of the PGET system was developed, including the test pipeline, collimator, and detector array. Projection data were obtained using the Geant4 Monte Carlo method. Image reconstruction was performed using the Algebraic Reconstruction Technique (ART), Maximum-Likelihood Expectation-Maximization (MLEM), and Ordered-Subsets Expectation-Maximization (OSEM), and an edge extraction method is proposed. With a collimator length of 90 mm and hole diameter of 1.1 mm, the reconstructed images achieved a resolution of 1.5 mm.

Key words: Lead-bismuth coolant; Corrosion; Passive gamma emission tomography.

1. Introduction

Lead-cooled fast reactors (LFRs) have been extensively researched in several countries [1–5] and are recognized as one of the most promising reactor types by the Generation IV International Forum [6] . Lead-bismuth eutectic (LBE), known for its high safety, economic advantages, and favorable neutron properties, is a key coolant choice for fast reactors. However, the use of LBE technology faces several challenges, one of which is its corrosive nature, which can compromise the integrity of structural materials [7]. Corrosion studies show that structural steel in direct contact with high-temperature, high-flow liquid LBE can corrode at rates of up to 1 mm/year for common stainless steels [8, 9] . An effective and economical method to mitigate corrosion is to maintain a protective oxide layer on the surface of the structural steel. This requires controlling the oxygen concentration in the LBE within a specific range. When the oxygen concentration is high, prolonged exposure (over 5000 hours) to LBE can lead to a thickening of the oxide layer. However, at high temperatures (above 500°C) and high flow rates, the flow-accelerated corrosion

(FAC) effect can cause the oxide layer to detach due to erosion. The detached oxide then flows with the LBE, leading to erode and further erosion of the structural steel. More seriously, this can block narrow channels in the reactor, potentially affecting the safe operation of the reactor [10]. Therefore, it is essential to develop a non-destructive testing method for the corrosion test of the lead-bismuth coolant pipeline.

Non-destructive testing (NDT) refers to techniques used to evaluate defects, the extent of damage, and the location of issues in an object without compromising its integrity. Common NDT methods for pipelines include ultrasonic testing [11], eddy current testing [12], and industrial computed tomography (ICT) [13]. However, due to the high density of the lead-bismuth material, ultrasonic testing thus has low resolution. Eddy current testing is also less effective for detecting internal defects in thick components. Among these, ICT is the most promising non-invasive method for revealing defects on the inner walls of pipelines. Yet, due to the high absorption of lead-bismuth, this method requires high-energy X-rays or neutron sources. In addition, it is difficult to rotate the lead-bismuth coolant around the central axis.

Based on ICT testing methods, this paper proposes the use of passive gamma emission tomography (PGET) to inspect lead-bismuth coolant pipelines. As LBE flows through the reactor core, the elements of Pb and Bi may be activated by neutrons. Activated nuclides in LBE can emit Gama rays. We may establish PGET detector arrays outside the pipeline to get activity image of the LBE in the pipeline. These images can provide detailed information about the contact surface between the pipeline and the LBE. If the pipeline is corroded by the coolant, the LBE will fill the corroded areas, leading to changes in the activity image that reflect the corrosion. In contrast to the ICT, the PGET method does not require the use of an external radioactive source or the rotation of the source around its axis.

The PGET method was first proposed by Levai et al. [14], and its feasibility was subsequently studied. With support from the International Atomic Energy Agency, the European Commission established a PGET system for nondestructive testing of spent fuel assemblies [15]. This system was later upgraded with new detectors and electronics [16]. It has since been used for data measurement at the VVER-440/213 reactor at the Loviisa nuclear power plant and the SVEA-96 reactor at the Olkiluoto nuclear power plant [17]. Similar systems for testing spent fuel components have also been developed in countries such as Korea, Sweden, and Norway [18–20]. However, to date, no reports have been found regarding the application of this method to test lead-bismuth coolant pipelines.

This paper investigates the feasibility of using the PGET method for NDT of corrosion in lead-bismuth coolant pipelines. With Geant4 Monte Carlo method, we get projection data,and use algorithms to recunstrute image. Through image quality analysis, we identify better algorithms and collimator parameters. We hope that this work can provide a reference for the development of PGET systems for LBE.

2. Monte Carlo simulation

2.1 PGET setup

As shown in **Figure 1**, the PGET setup in Geant4 consists of a lead-bismuth coolant pipeline, two collimators, and two detector arrays. The LBE is composed of 55.5% bismuth and 44.5% lead [21]. The structural material of the pipeline is 316L steel, with an outer diameter of 70 mm and an inner diameter of 60 mm. To simulate corrosion in the pipeline, eight spherical defects are introduced along the contact surface

between the pipeline and the LBE. The radii of the defects are 4.5 mm, 4.0 mm, 3.5 mm, 3.0 mm, 2.5 mm, 2.0 mm, 1.5 mm, and 1.0 mm, respectively.

The tungsten-copper collimator features a hole-type structure, with a 10 mm spacing between adjacent holes. The length of holes is l_c and the diameter d. The collimator is positioned 70 mm from the center of the object. To increase the amount of projection data, the two detector arrays are offset by 1 mm. Each detector array consists of 10 Bismuth Germanate (BGO) detectors, with a diameter of 6 mm and a length of 10 mm. The BGO detectors are shielded by a 2 mm layer of tungsten-copper alloy.

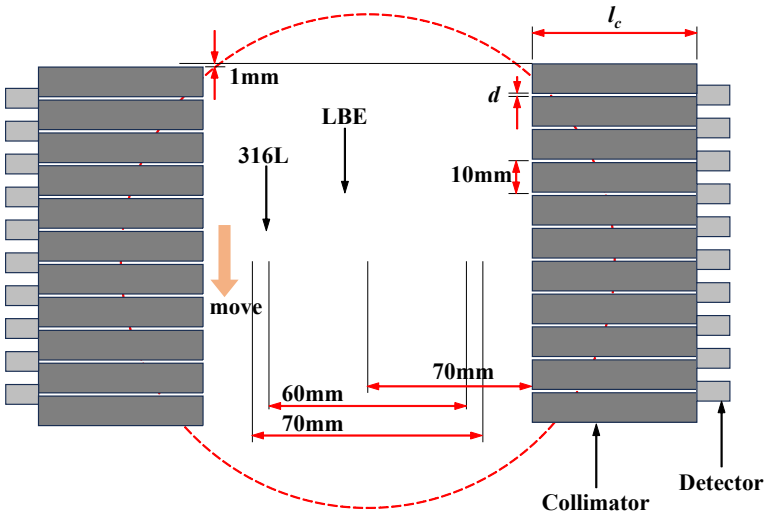

Figure 1 Schematic diagram of PGET setup.

2.2 Radiation source

The main gamma-emitters in the coolant with the operation of LFR are radionuclides of: ^{207m}Pb, ^{204m}Pb and ^{203}Pb [22]. Due to its short half-life of 0.806s, ^{207m}P can be neglected. The primary radionuclides used for simulation are ^{204m}Pb and ^{203}Pb, as summarized in the **Table 1**. These radionuclides are assumed to be uniformly distributed in the LBE.

Table 1 Simulated radionuclides parameters.

Radionuclides	Half-life	Activity (Bq/kg)	Energy(keV)	Branching ratio (%)
^{204m}Pb	66.93m	6.56×10^{10}	899.15	99.174
			911.74	91.5
			374.76	94.20
^{203}Pb	51.92h	2.98×10^{9}	279.20	80.94

2.3 Monte Carlo simulation

In the Monte Carlo simulation, the object can rotate 360° around its center with a step size of 1°. (1)At each angle, a projettion data is gotton by simulation. (2)When the object rotated 360°, we move the collimators 2 mm perpendicular to the collimator hole, and repeat (1). And then, move collimators in steps of 2 mm, 4 times, repeat (1) and (2). Thus,we can get 1800 projection data. For each projection data,we simulates 1×10^9

Gama photons emitting from LBE. The energy resolution of the BGO detectors is not good [23], therefore, only the total events for the detector within the full energy window are recorded.

3. Results and discussion

3.1 Image reconstruction

The image reconstruction method of PGET is similar to that of single-photon emission computed tomography (SPECT) [18], aiming to obtain the activity image of the object. The commonly used algorithms for tomographic image reconstruction are classified into analytical and iterative methods. The analytical method relies on inverse solving formulas, making it simple to implement and fast to compute. The iterative method is based on solving linear equations and is particularly suited for scenarios where attenuation distribution must be considered, so it is employed in this paper. Common iterative algorithms include the algebraic reconstruction technique (ART) [24], maximum-likelihood expectation-maximization (MLEM) [25], and ordered-subsets expectation-maximization (OSEM) [26]. For iterative algorithms, the iteration times have a significant impact on the quality of the reconstructed image. **Figure 2** shows the reconstructed images obtained using three iterative algorithms at different iteration counts. The reconstructed image has a resolution of 200 × 200 pixels, with each pixel measuring 0.5 mm × 0.5 mm.

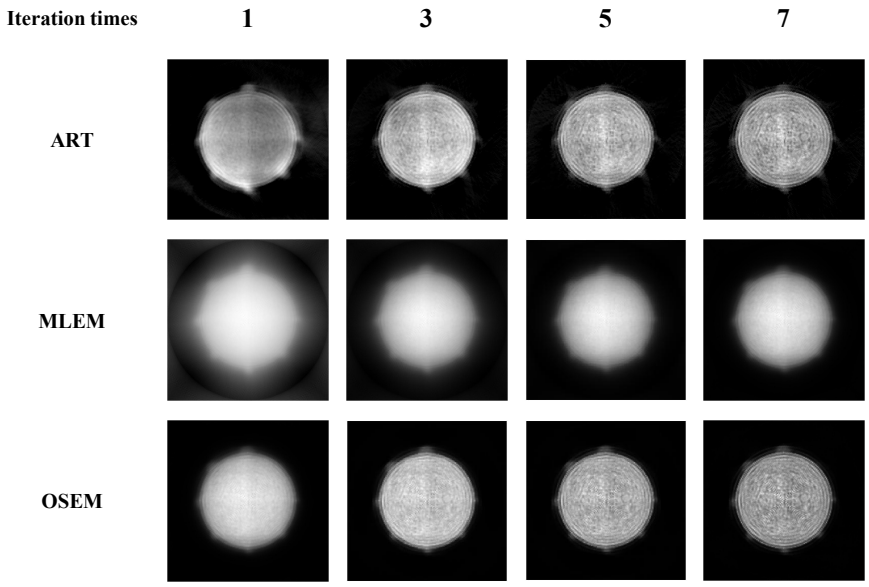

Figure 2 Reconstructed image of three iterative algorithms with different iteration times.

3.2 Edge extraction and Image quality assessment

We focus on the corroded interface between LBE and 316L pipeline, therefore, we investigate a method for extracting edges from activity images. As shown in **Figure 3** (a), the red line passing through the center of the reconstructed image, if the value of the pixel point exceeds the preset threshold *t*, the pixel point value is considered as LBE. The center-to-edge distance of LBE for each angle can be obtained by rotating counterclockwise in 1° increments from the red line, as shown in the following equation:

$$D(\theta) = \sum_{j=1}^{F_\theta(j)<t} R_\theta(j) \#(1)$$

where $D(\theta)$ represents the center-to-edge distance at angle θ, $R_\theta(j)$ represents the length of the j-th pixel point at angle θ, $F_\theta(j)$ represents the value of the j-th pixel point at angle θ, t represents the threshold.

Similarly, the center-to-edge distance of the standard image can be obtained using the Monte Carlo model. A comparison of the center-to-edge distances between the standard image and the reconstructed image with different t is shown in **Figure 3** (b). It is evident that the threshold t significantly influences the results of edge extraction.

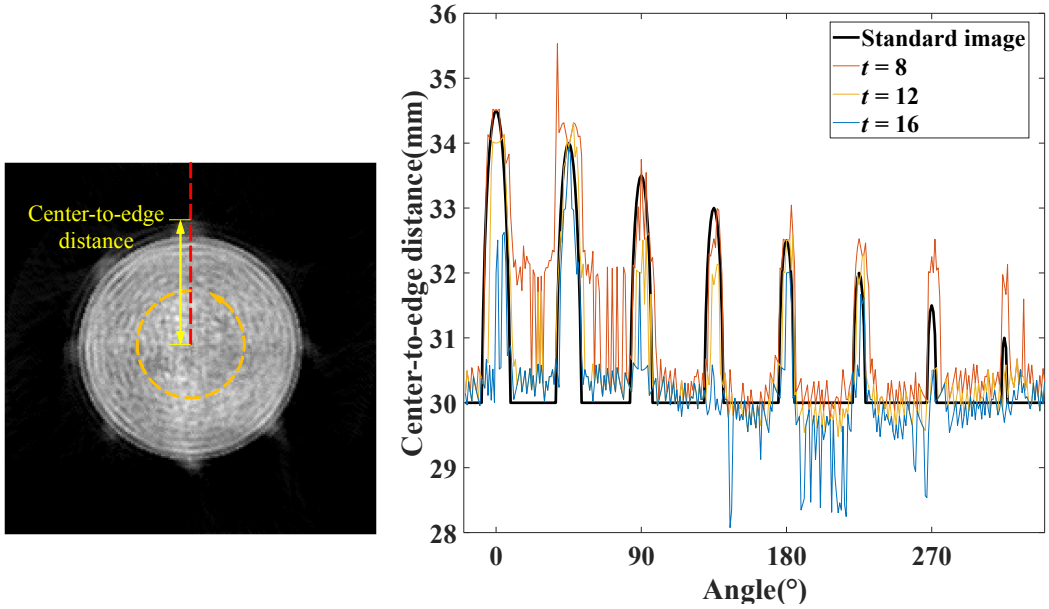

(a) (b)

Figure 3 (a) Edge extraction method. (b) Center-to-edge distance of standard image and reconstructed image with different t by ART of 5 iterations.

To determine the optimal threshold and assess image quality, a quantitative analysis of the edges in the reconstructed image is necessary. The Mean Squared Error (MSE) [27] is used to evaluate the similarity in the center-to-edge distance between the reconstructed image and the standard image, and is calculated as follows:

$$\mathrm{MSE} = \frac{1}{MN} \sum_{x=1}^{N} \sum_{y=1}^{M} [I_s(x, y) - I_r(x, y)]^2 \#(2)$$

where M and N represent the length and width of the image, x and y represent pixel point positions of the image, I_s represents the center-to-edge distance of standard image, and I_r represents the center-to-edge distance of reconstructed image. The smaller the MSE, the better the image quality.

The optimal threshold is determined by minimising the MSE of the image. Once the optimal threshold is found, the edge pixels at each angle are highlighted using this threshold, resulting in the edge-extracted image,

as shown in **Figure 4** (a). A comparison of the standard image and reconstructed image with optimal threshold are shown in **Figure 4** (b).

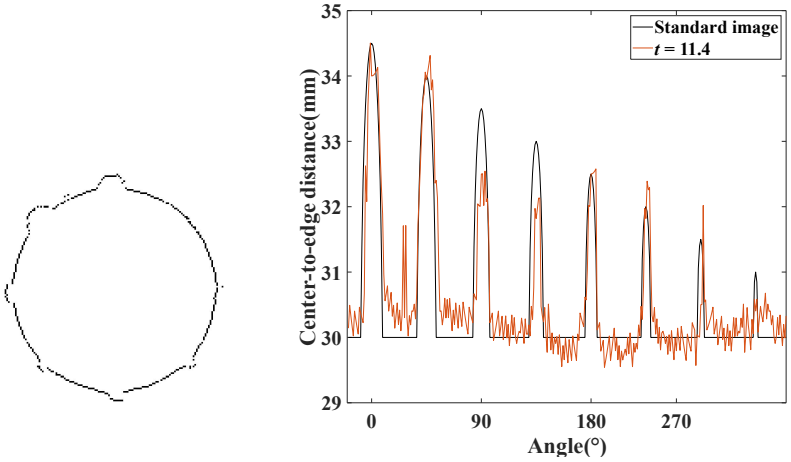

(a) (b)

Figure 4 (a) Edge-extracted image. (b) Center-to-edge distance of standard image and reconstructed image with optimal threshold (t =11.4) by ART of 5 iterations.

3.3 Effect of algorithms on image quality

The edge-extraction image of three iterative algorithms with different iteration times are shown in **Figure 5**. the reconstructed image from the MLEM method exhibits relatively poorer edge information after the same iteration times compared to ART and OSEM. With same iteration times, ART produces more image artifacts and the minimum resolution of the image is poor, and OSEM produces better image quality.

The effect of ART, MLEM, and OSEM with different iteration times on the MSE is shown in **Figure 6**. Clearly, at the same iteration times, the images reconstructed using OSEM converge more quickly and are more similar to the standard image. Therefore, we conclude that OSEM provides the best image reconstruction results in this study. Given that the MSE after 5 iterations with OSEM is relatively stable, we use OSEM with 5 iterations for subsequent reconstructions.

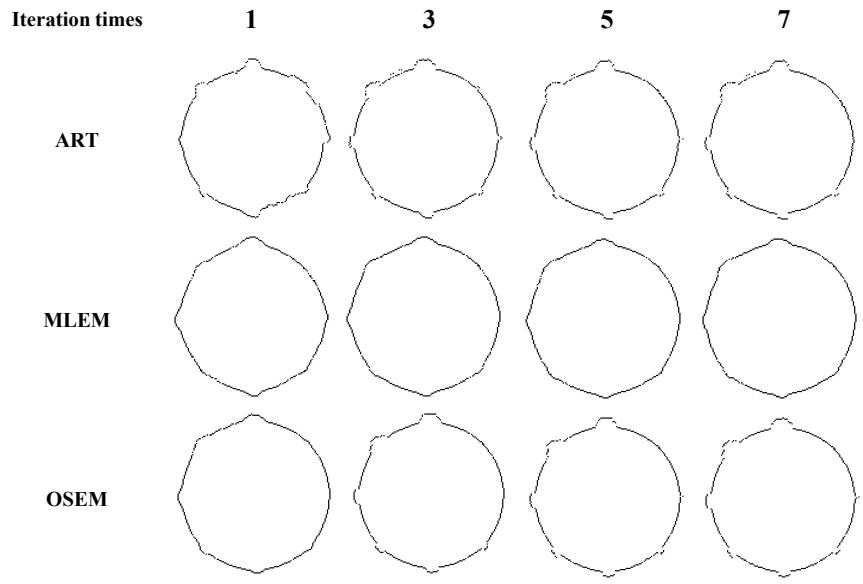

Figure 5 Edge-extraction image of three iterative algorithms with different iteration times.

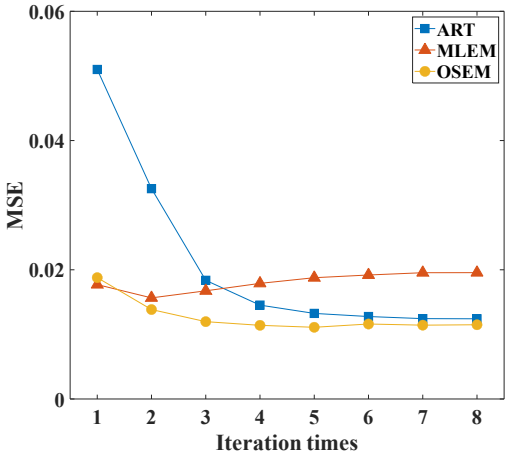

Figure 6 Effect of ART, MLEM and OSEM with different iteration times on MSE.

3.4 Effect of collimator geometry on image quality

Once the spacing between the holes of the collimator is determined, the image quality is primarily influenced by the collimator length and hole diameter. A longer collimator and smaller hole diameter result in higher spatial resolution. The MSE of reconstructed images with seven different collimator lengths and eight different collimator hole diameters are shown in **Figure 7**.

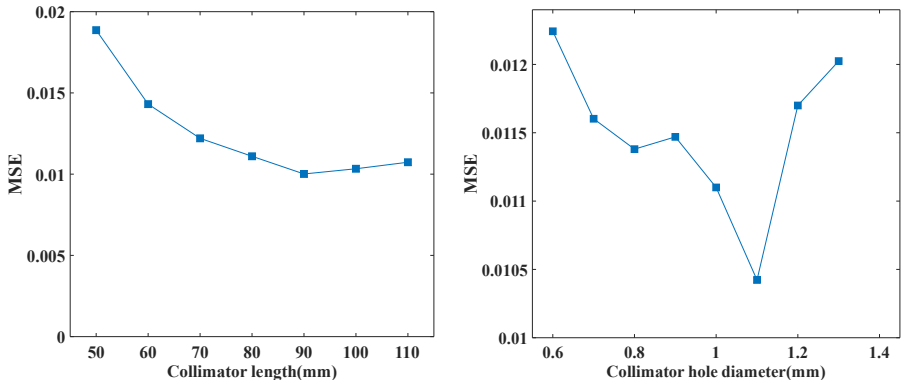

(a) (b)

Figure 7 (a) Effect of different collimator length on MSE. (b) Effect of different collimator hole diameter on MSE.

As the collimator length increases, the number of scattered particles detected decreases, leading to reduced image noise and improved image quality. When the collimator length increases, the MSE shows an upward trend, stabilizing once the length exceeds 90 mm. Therefore, a collimator length of 90 mm is considered better. A smaller collimator hole diameter results in lower detection efficiency, while a larger hole diameter reduces spatial resolution, both of which contribute to a higher MSE. Since the MSE reached its minimum value at a collimator hole diameter of 1.1 mm, a hole diameter of 1.1 mm is considered better.

By analyzing the effect of collimator geometry parameters on image quality, we optimized the collimator to a length of 90 mm and a hole diameter of 1.1 mm. After optimization, the reconstruction image and edge-extraction image using OSEM are shown in **Figure 8**, while the center-to-edge distance of the

standard and reconstructed images is shown in **Figure 9**. The reconstructed image exhibits fewer artifacts, better noise resistance, and a minimum resolution of 1.5 mm.

Considering the absolute error between the reconstructed image and the standard image, the error is less than 1.0 mm at locations without corrosion. The error at corroded locations is less than 1.5 mm, with only a few exceptions. This indicates that the positional resolution of the image is below 1.5 mm.

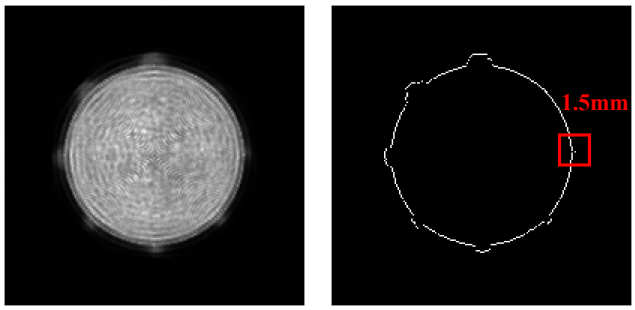

(a) (b)

Figure 8 (a) Reconstruction images of optimized collimator. (b) Edge-extraction image of optimized collimator.

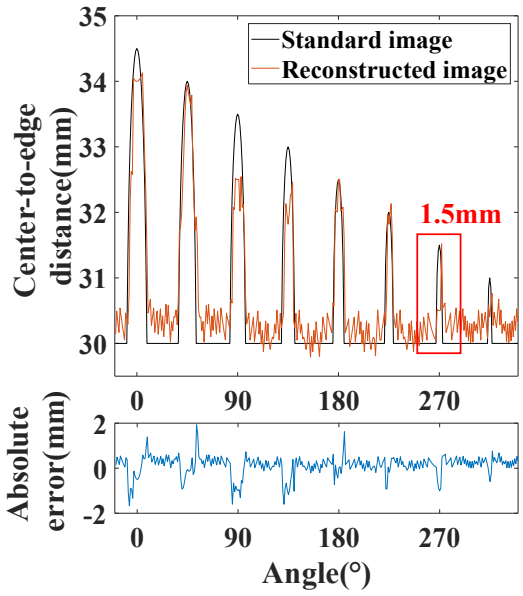

Figure 9 Center-to-edge distance of standard image and reconstructed image with the optimized collimator is calculated, and the absolute error is obtained.

4. Conclusion

In this paper, we investigate the feasibility of using the PGET method for corrosion detection of lead-bismuth coolant pipelines, employing the Geant4 Monte Carlo method. An edge extraction method is proposed, and the reconstruction results effectively highlight the corrosion in the pipeline. The OSEM method has a better image quality compared to ART and MLEM. By comparing the quality of the reconstructed images, we optimized the collimator parameters to a length of 90 mm and a hole diameter of 1.1 mm. With the optimized collimator, the image resolution is improved to below 1.5 mm.

Next, we will enhance both the device and algorithms to further improve image resolution. We also plan to use the optimized collimator parameters in the construction of the PGET device. We anticipate that this PGET-based testing method will significantly improve the efficiency and resolution for detecting corrosion in lead-bismuth coolant pipelines, compared to traditional NDT methods.

Acknowledgments:

We thank Nuclear Power Institute of China for joint innovation fund sponsorship.

References:

[1] T. Mukaiyama, H. Takano, T. Ogawa, T. Takizuka and M. Mizumoto, *Partitioning and transmutation studies at JAERI both under OMEGA program and High-Intensity Proton Accelerator Project*, *Progress in Nuclear Energy* **40**, (2002) 403.

[2] J. J. Sienicki, A. Moisseytsev, W. S. Yang, D. C. Wade, A. Nikiforova, P. Hanania, H. J. Ryu, K. P. Kulesza, S. J. Kim, et al., *Status Report on the Small Secure Transportable Autonomous Reactor (SSTAR) /Lead-Cooled Fast Reactor (LFR) and Supporting Research and Development.*, United States, (2008).

[3] D. De Bruyn, A. Alemberti, L. Mansani, G. Grasso, C. Artioli, E. Bubelis, G. Mueller, J. Wallenius and A. Orden, *Main Achievements of the FP7-LEADER Collaborative Project of the European Commission Regarding the Design of a Lead-Cooled Fast Reactor*, (2013).

[4] E. O. Adamov, A. V. Kaplienko, V. V. Orlov, V. S. Smirnov, A. V. Lopatkin, V. V. Lemekhov and A. V. Moiseev, *Brest Lead-Cooled Fast Reactor: From Concept to Technological Implementation*, *Atomic Energy* **129**, Springer, (2021) 179.

[5] I. S. "Hwang E-mail: hisline@snu.ac.kr [Seoul National University Department of Nuclear Engineering Seoul (Korea Republic of)" and E. R. C. of K.-N. (Korea "Nuclear Transmutation Republic of)]," *PEACER [Proliferation-Resistant Environment-Friendly Accident-Tolerant Continual Economical Reactor] PEACER*, IAEA, (2007).

[6] J. E. Kelly, *Generation IV International Forum: A decade of progress through international cooperation*, *Progress in Nuclear Energy* **77**, Elsevier Ltd, (2014) 240.

[7] E. Serag, B. Caers, P. Schuurmans, S. Lucas and E. Haye, *Challenges and coating solutions for wear and corrosion inside Lead Bismuth Eutectic: A review*, in *Surf Coat Technol* **441**, Elsevier B.V., (2022).

[8] J. Zhang and N. Li, *Parametric study of a corrosion model applied to lead-bismuth flow systems*, *Journal of Nuclear Materials* **321**, (2003) 184.

[9] J. Zhang, *A review of steel corrosion by liquid lead and lead-bismuth*, in *Corros Sci* **51**, (2009).

[10] A. V. Zrodnikov, V. I. Chitaykin, B. F. Gromov, O. G. Grigoryv and A. V Dedoul, *USE OF RUSSIAN TECHNOLOGY OF SHIP REACTORS WITH LEAD-BISMUTH COOLANT IN NUCLEAR POWER*, (2004).

[11] Y. Hatsukade, N. Masutani, S. Teranishi, K. Masamoto, S. Kanenaga, S. Adachi and K. Tanabe, *HTS-SQUID NDE Technique for Pipes Based on Ultrasonic Guided Wave*, in *J Phys Conf Ser* **871**, Institute of Physics Publishing, (2017).

[12] J. B. Nestleroth and R. J. Davis, *Application of eddy currents induced by permanent magnets for pipeline inspection*, *NDT and E International* **40**, (2007) 77.

[13] B. DENG, X. YU, A. LI and H. XU, *Nondestructive analysis by combined X-ray tomography on a synchrotron radiation facility*, *Nuclear Science and Techniques* **18**, (2007) 257.

[14] F. Lévai, S. Dési, Sz. Czifrus, S. Feher, M. Tarvainen, T. Honkamaa, J. Saarinen, M. Larsson, A. Rialhe, et al., *FEASIBILITY OF GAMMA EMISSION TOMOGRAPHY FOR PARTIAL DEFECT VERIFICATION OF SPENT LWR FUEL ASSEMBLIES*, (2002).

[15] T. Honkamaa, F. Levai, R. Berndt, P. Schwalbach, S. Vaccaro and A. Turunen, *A Prototype for Passive Gamma*

Emission Tomography, (2014).

[16] T. White, M. Mayorov, N. Deshmukh, E. Miller, L. E. Smith, J. Dahlberg and T. Honkamaa, *SPECT Reconstruction and Analysis for the Inspection of Spent Nuclear Fuel*, in *2017 IEEE Nuclear Science Symposium and Medical Imaging Conference (NSS/MIC)*, (2017).

[17] C. Belanger-Champagne, P. Peura, P. Eerola, T. Honkamaa, T. White, M. Mayorov and P. Dendooven, *Effect of Gamma-Ray Energy on Image Quality in Passive Gamma Emission Tomography of Spent Nuclear Fuel*, *IEEE Trans Nucl Sci* **66**, Institute of Electrical and Electronics Engineers Inc., (2019) 487.

[18] H. Kim, M. Lee, H. Choi, C. Min and H. Choi, *Tomographic Image Reconstruction Techniques for Accurate Spent Fuel Assembly Verification*, in *Journal of Instrumentation* **18**, Institute of Physics, (2023).

[19] P. Jansson, S. Jacobsson Svärd, A. Håkansson and A. Bäcklin, *A device for nondestructive experimental determination of the power distribution in a nuclear fuel assembly*, *Nuclear Science and Engineering* **152**, (2006) 76.

[20] S. Holcombe, S. Jacobsson Svärd and L. Hallstadius, *A Novel gamma emission tomography instrument for enhanced fuel characterization capabilities within the OECD Halden Reactor Project*, *Ann Nucl Energy* **85**, Elsevier Ltd, (2015) 837.

[21] X. Gong, M. P. Short, T. Auger, E. Charalampopoulou and K. Lambrinou, *Environmental degradation of structural materials in liquid lead- and lead-bismuth eutectic-cooled reactors*, in *Prog Mater Sci* **126**, Elsevier Ltd, (2022).

[22] International Atomic Energy Agency., *Liquid Metal Coolants for Fast Reactors Cooled by Sodium, Lead, and Lead-Bismuth Eutectic.*, International Atomic Energy Agency, (2012).

[23] H. J. Choi, I. S. Kang, K. B. Kim, Y. H. Chung and C. H. Min, *Optimization of single-photon emission computed tomography system for fast verification of spent fuel assembly: A Monte Carlo study*, *Journal of Instrumentation* **14**, Institute of Physics Publishing, (2019).

[24] H. Lee, S. Choi, D. Lee, Y. -s. Kim, H.-S. Park, Y. Lee, C.-W. Seo and H.-J. Kim, *Investigation of various reconstruction parameters for algebraic reconstruction technique in a newly developed chest digital tomosynthesis*, *Journal of Instrumentation* **12**, (2017) P08016.

[25] J. ZHANG, Y. KONG, J. ZHOU, J. ZHANG, L. ZHANG, C. WANG, C. ZHU and B. LI, *Proportion of viable myocardium is more reliable than semi-quantitative score in predicting functional recovery: a pilot study of PET myocardial viability imaging*, *Nuclear Science and Techniques* **19**, (2008) 32.

[26] A. R. Yu, J. S. Kim, J. H. Kang and S. M. Lim, *Comparison of reconstruction methods and quantitative accuracy in Siemens Inveon PET scanner*, *Journal of Instrumentation* **10**, (2015) P04001.

[27] S. Bae, J. Bae, H. Lee and K. Lee, *Development of correction methods for variable pinhole single-photon emission computed tomography*, *Journal of Instrumentation* **11**, (2016) C02060.